arXiv:0904.4549v1 [quant-ph] 29 Apr 2009

Bose-Einstein condensates on tilted lattices: coherent, chaotic and subdiffusive dynamics

Andrey R. Kolovsky,[1] Edgar A. Gómez,[2, 3] and Hans Jürgen Korsch[2]

[1]*Kirensky Institute of Physics and Siberian Federal University, 660036 Krasnoyarsk, Russia*
[2]*Fachbereich Physik, Technische Universität Kaiserslautern, D-67653 Kaiserslautern, Germany*
[3]*Departamento de Física, Universidad Nacional de Colombia, Bogotá D.C., Colombia*

(Dated: April 29, 2009)

The dynamics of a (quasi)one-dimensional interacting atomic Bose-Einstein condensate in a tilted optical lattice is studied in a discrete mean-field approximation, i.e., in terms of the discrete nonlinear Schrödinger equation. If the static field is varied the system shows a plethora of dynamical phenomena. In the strong field limit we demonstrate the existence of (almost) non-spreading states which remain localized on the lattice region populated initially and show coherent Bloch oscillations with fractional revivals in the momentum space (so called quantum carpets). With decreasing field, the dynamics becomes irregular, however, still confined in configuration space. For even weaker fields we find sub-diffusive dynamics with a wave-packet width spreading as $t^{1/4}$.

PACS numbers: 03.75.Kk, 03.75.Nt

Recently much attention has been payed to Bloch oscillations (BO) of a Bose- Einstein condensate (BEC) of cold atoms in tilted optical lattices (see Refs. [1, 2, 3, 4, 5, 6, 7, 8, 9, 10, 11], to cite few of the relevant papers). The main question one addresses here, both experimentally and theoretically, is the effect of atom-atom interactions on the otherwise perfectly periodic atomic dynamics. Although all experiments on BEC's BO were done for a localized initial conditions, theoretically a simpler case of uniform initial conditions, where atoms are delocalized over whole lattice, is usually analyzed [3, 4, 5, 11]. It was found that depending on the system parameters a BEC of interacting atoms may show three different regimes of BO [11]: (i) exponentially decaying BO where the condensate rapidly decoheres, which corresponds to unstable (chaotic) BO in the mean-field approach; (ii) persistent BO and (iii) modulated BO, which both correspond to stable dynamics in the mean-field approach. Assuming the magnitude of a static field to be the control parameter, these three regimes refer to weak, moderate, and strong static fields, respectively.

In the present work we extend previous studies to the case of nonuniform initial conditions, realized in a laboratory experiment. In what follows we focus on the mean-field analysis, - a comparison with quantum mechanical treatment remains an open and challenging problem, as it will be discussed in some more detail in the concluding paragraph of the paper.

In the mean-field approximation, the dynamics of a BEC in a tilted optical lattice can be described by the discrete nonlinear Schrödinger equation (DNLSE)

$$i\,\hbar\dot{a}_l = dFla_l - \frac{J}{2}(a_{l+1}+a_{l-1}) + g|a_l|^2 a_l \qquad (1)$$

where a_l is the BEC complex amplitude in the lth potential well. The static force F leads to a linear increase of the onsite energy dFl (d is the lattice period), J measures the tunneling transitions between the wells and g characterizes the atomic interaction. Equation (1) appears as a canonical equation of motion $i\,\hbar\dot{a}_l = \partial H/\partial a_l^*$, $i\,\hbar\dot{a}_l^* = -\partial H/\partial a_l$ of a 'classical' Hamiltonian function

$$H = \sum_l dFl\,|a_l|^2 - \frac{J}{2}\sum_l\left(a_{l+1}^* a_l + c.c.\right) + \frac{g}{2}\sum_l |a_l|^4\,. \qquad (2)$$

The norm $\sum_l |a_l|^2$ is conserved under the evolution and we assume $\sum_l |a_l|^2 = 1$ in the following (which assumes that g is proportional the number of atoms), as well as units where $\hbar = 1$ and $d = 1$.

The gauge transformation $a_l(t) \rightarrow \exp(-iFlt)a_l(t)$ converts the static term in Eq. (1) into a periodic driving with the Bloch frequency F,

$$i\dot{a}_l = -\frac{J}{2}\left(e^{-iFt}a_{l+1} + e^{+iFt}a_{l-1}\right) + g|a_l|^2 a_l\;, \qquad (3)$$

and a Fourier transform of the amplitudes a_l yields the Bloch-waves representation $b_k = \frac{1}{\sqrt{L}}\sum_{l=1}^{L}\exp(-i\kappa l)\,a_l$, where $\kappa = 2\pi k/L$ is the quasimomentum ($-\pi \le \kappa < \pi$). As follows from (3), the amplitudes b_k obey the equation

$$i\dot{b}_k = -J\cos(\kappa - Ft)b_k + \frac{g}{L}\sum_{k_1,k_2,k_3} b_{k_1}b_{k_2}b_{k_3}^*\tilde{\delta}(k_1+k_2-k_3-k) \qquad (4)$$

where $\tilde{\delta}(k)$ is the Kronecker function modulo L. It is easy to see that the displayed equations of motion can be solved in closed form in the case of uniform initial conditions, $a_l(0) = const$, yielding $b_0(t) \sim \exp\left(i\frac{J}{F}\sin(Ft) - i\frac{g}{L}t\right)$ and $b_{k\neq 0}(t) \equiv 0$, i.e. ordinary BO. The stability of this solution with respect to weak perturbations has been analyzed in Ref. [4, 5], also in comparison with related phenomena in the many-particle Bose-Hubbard model for a small number of particles and lattice sites [11].

Motivated by recent experiments [10], where a BEC of Cesium atoms was prepared in a harmonic trapping potential in the Thomas-Fermi regime, we chose a Thomas-Fermi distribution

$$a_l(0) = \sqrt{\beta - \alpha l^2} \qquad (5)$$

for $\alpha l^2 < \beta$ and zero otherwise. We shall use $\alpha = 0.001$, which populates lattice sites between $l = -9$ and $l = +9$ (the value of β is fixed by normalization). The results of a numerical solution of the nonlinear coupled equations (3) with initial conditions (5) and parameters $J = 1$, $g = 10$ are presented in Figs. 1 and 2 as a function of time measured in units of $T_{\rm rev}$ as defined in Eq. (8) below. The site populations $P_l(t) = |a_l(t)|^2$ are shown in the upper panel and the quasimomentum distributions $|b_k|^2$ in the lower panels. When the force F is varied, one observers a characteristic transition from a highly coherent evolution for strong fields to an irregular chaotic motion for intermediate fields and a nonlinear diffusion for weak fields. In the following sections we will discuss the dynamics in the three different regimes in some detail.

Coherent evolution. For strong fields, as in the case $F = 100$ shown in Fig. 1, the lattice population $P_l(t) = |a_l(t)|^2$ is almost frozen without observable structure. On the contrary, the quasimomentum distribution shows a highly organized pattern, also denoted as a quantum carpet. The initial distribution is reconstructed at time $T_{\rm rev}$, the revival time, and at rational ratios of $t/T_{\rm rev}$ we find fractional revivals. Such highly organized patterns have been observed recently experimentally for BECs in tilted optical lattices [10].

The origin of these quantum carpets lies in the initial distribution (5). Indeed, in the limit $F \to \infty$ the site populations are constant [11], $|a_l(t)| \approx |a_l(0)|$, and the phases evolve linearly in time:

$$a_l(t) \approx a_l(0) \exp\left[-ig|a_l(0)|^2\, t\right] \qquad (6)$$

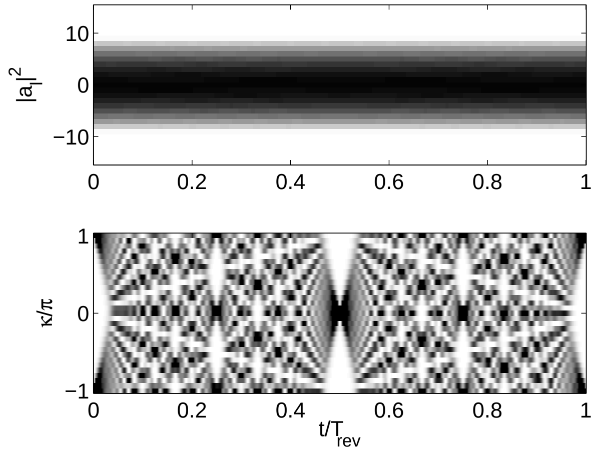

FIG. 1: Lattice site populations $P_l(t) = |a_l(t)|^2$ (upper panel) and the quasimomentum distribution (lower panel) as a function of time in unites of the revival time $T_{\rm rev} = 2\pi/g\alpha$ for a force $F = 100$ (parameters $g = 10$, $J = 1$). The site populations are frozen and the quasimomentum distribution show a highly organized quantum carpet structure.

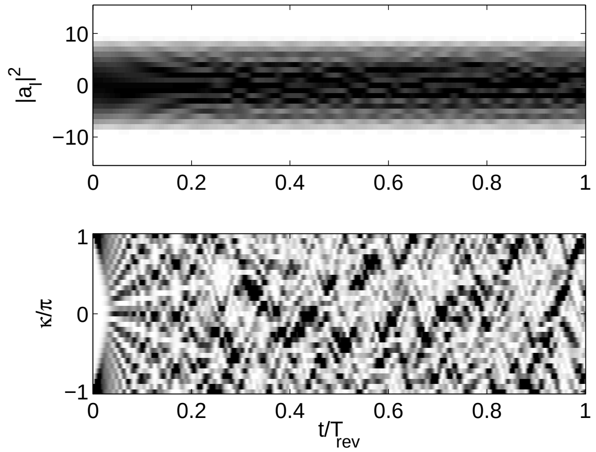

FIG. 2: Same as Fig. 1, however for a weaker force $F = 10$. The site populations are still localized but show fluctuations. The quasimomentum distribution appears to be irregular after a transient time.

(see also [7]). In the Bloch-wave representation we find

$$b_k \sim \exp(-ig\beta t) \sum_l \exp\left[i(\kappa l + g\alpha l^2 t)\right], \quad k = 0, \pm 1, \dots, \qquad (7)$$

an expression already given in [10]. The most prominent feature of such Gaussian sums, which have been analyzed in much detail during recent years (see, e.g., [12, 13, 14, 15, 16]) are the revivals and fractional revivals. From Eq. (7) the revival time is given by

$$T_{\rm rev} = 2\pi/g\alpha \qquad (8)$$

in agreement with the numerical results shown in Fig. 1 for $F = 100$. In comparison with the Bloch period $T_{\rm B} = 2\pi/F$ we have $T_{\rm rev}/T_{\rm B} = F/g\alpha = 10^4$, i.e. the revival time is much larger than the Bloch period. For rational fractions $t/T_{\rm rev} = m/n$ (n, m integer), there appear n (approximate) copies of the initial distribution of reduced size. For irrational ratios we find fractal distributions [13].

It should, however, be pointed out that the limiting strong field behavior in Eqs. (6) and (7) describes the evolution for finite values of F only approximately and the coherent evolution shown in Fig. 1 is a transient phenomenon for intermediate forces. For $F = 10$, as shown in Fig. 2, the quantum carpets gradually disappear after a time interval $T_{\rm coh} \approx 0.2\, T_{\rm rev}$ for $F = 10$. This coherence time was found to vary approximately linear with F.

Chaotic evolution. The distortion of the quantum carpets in the quasimomentum distribution for $t > T_{\rm coh}$ is accompanied by fluctuations in the site populations $P_l(t)$. However, lattice populations are still entirely localized on the initial interval and fluctuate around the initial population $P_l(0)$. A measure for these fluctuations is given by the quantity $C(t) = \sum_l \left|P_{l+1}(t) - P_l(t)\right|$, which saturates

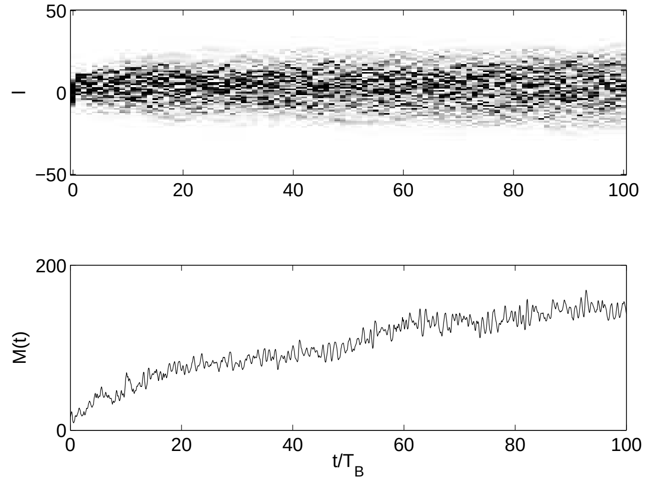

FIG. 3: Site populations $P_l(t)$ (upper panel) and dispersion $M(t)$ (lower panel) as a function of time in units of the Bloch period $T_\mathrm{B} = 2\pi/F$ for $F = 0.25$. The other parameters are the same as in Figs. 1, 2 except the upper limit of the time axis, which is four times larger.

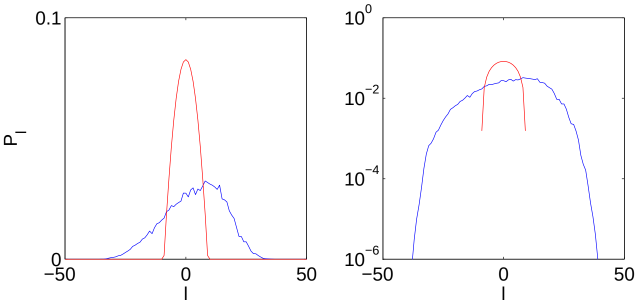

FIG. 4: Distributions of site populations P_l at the end of the numerical simulation discussed in Fig. 3 (blue solid line) compared to the initial distribution (red solid line) on linear (left panel) and logarithmic (right panel) scales.

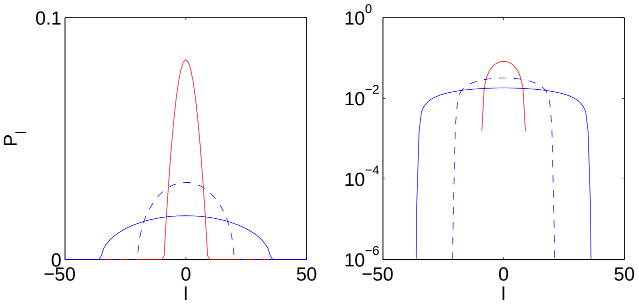

FIG. 5: Solution of the nonlinear diffusion equation for $\widetilde{D} = 50$ on linear (left panel) and logarithmic (right panel) scales. Distributions at $t = 0$ (red solid lines), $t/2\pi = 100$ (blue dashed lines), and $t/2\pi = 1000$ (blue solid lines) are shown.

in time on a level, which increases strongly with decreasing F. This behavior of $C(t)$ may serves as an indicator the transition from regular to irregular dynamics.

An alternative indicator of this transition is the finite time Lyapunov exponent

$$\lambda(t) = \ln|\delta\mathbf{a}(t)|/t\ , \tag{9}$$

where $\delta\mathbf{a}(t)$ evolves in the tangent space according to the linear equation

$$i\frac{d\delta\mathbf{a}}{dt} = \mathcal{M}[\mathbf{a}(t)]\,\delta\mathbf{a}(t)\,, \tag{10}$$

where $\mathcal{M}$ is the Jacobian matrix of the evolution equation (3). We have found that for moderate and weak fields, the finite time Lyapunov exponent converges to a positive value after approximately ten Bloch periods, which indicates a chaotic motion. For strong fields $F \geq 10$ the finite time Lyapunov exponent behaves as $1/t$ during the whole simulation time period [17].

Nonlinear diffusion. As mentioned above, for a weak field the dynamics of the system is chaotic with no sign of the quantum carpet in the quasimomentum distribution and erratic evolution of the site populations. This regime is depicted in the upper panel of Fig. 3, where one notices an additional effect not present in Figs. 1, 2 – the wave packet spreading. More quantitatively this can be seen in the lower panel, which displays the dispersion $M(t) = \sum_l l^2 P_l - (\sum_l l P_l)^2$ of the population distribution. A closer analysis of the functional dependence of $M(t)$ reveals a $\sqrt{t}$-law with the prefactor increasing with decrease of the static field magnitude. In addition to Fig. 3 and for purposes of future reference, Fig. 4 shows the distribution of the site populations P_l at the end of the numerical simulations where, to reduce fluctuations of $P_l(t)$, they are averaged over the last 25 Bloch periods.

A qualitative explanation for the observed subdiffusive spreading is as follows. In view of the apparently random behavior of $P_l(t)$ we replace in Eq. (3) the squared amplitudes $|a_l(t)|^2$ in the interaction term by a random variable, $|a_l(t)|^2 \sim \xi(t)$, with an exponentially decaying correlation function

$$R(t-t') = \overline{\xi(t)\xi(t')} = \overline{\xi^2}\exp(-|t-t'|/\tau)\ .$$

Assuming the quantity $\overline{\xi^2} \sim \overline{|a_l(t)|^4}$ in the last equation to be independent of l, this leads to a diffusive spreading of the distribution according to the discrete diffusion equation [18]

$$\dot{P}_l = D\,(P_{l+1} - 2P_l + P_{l-1}) \tag{11}$$

where the diffusion coefficient D is given by

$$D = \gamma/(F^2+\gamma^2) \approx \gamma/F^2 \quad \text{with} \quad \gamma = \overline{\xi^2}\tau\ . \tag{12}$$

(Note that Eq. (11) is a discretization of the continuous diffusion equation $\partial P/\partial t = D\partial^2 P/\partial x^2$ and conserves the norm $\sum_l P_l = 1$.) Since in the present case the quantities $\overline{|a_l(t)|^4} = P_l^2(t)$ depend on l, it is plausible to assume that the diffusion coefficient locally depends on l as $D(l) = \tilde{D}P_l^2(t)$. Then the site populations P_l obey a nonlinear diffusion equation

$$\dot{P}_l = \widetilde{D}\left(P_{l+1}^3 - 2P_l^3 + P_{l-1}^3\right) . \qquad (13)$$

This equation can be considered as a discretization of the continuous nonlinear diffusion equation

$$\frac{\partial P}{\partial t} = \widetilde{D}\frac{\partial}{\partial x}P^\nu \frac{\partial P}{\partial x} , \quad \text{for} \quad \nu = 2 , \qquad (14)$$

which appears, for example, in the problem of gas diffusion in a porous media [19]. For the considered case $\nu = 2$ one of the exact solutions of Eq. (14) is a semicircular distribution with a radius growing as $t^{1/4}$, which implies that the second momentum increases as $M(t) \sim \sqrt{t}$.

The discrete nonlinear diffusion equation (13) seems to inherit properties of its continuous counterpart, although we are not aware of any formal proof of this statement. As an example, Fig. 5 shows the result of numerical solution of Eq. (13) for the initial Thomas-Fermi distribution. Note, that asymptotically the solution is insensitive to the particular shape of the initial distribution and one gets the same result, for example, for a Gaussian of the same width.

A comparison between Fig. 4 and Fig. 5 shows that there are deviations of the actual profile for the site populations from that predicted by the nonlinear diffusion model (13). Nevertheless, the model (13) is capable to capture some essential features of the system dynamics, in particular, the $t^{1/4}$-law for the wave-packet spreading.

In conclusion, we have considered Bloch dynamics of a BEC in tilted optical lattices for the Thomas-Fermi initial profile, a typical initial condition in a laboratory experiment. Similar to the case of uniform initial conditions studied earlier, the system dynamics is found to strongly depend on the magnitude of a static field: it is regular in the strong field limit and chaotic in the weak field limit. In the former case of regular dynamics the BEC wave packet is frozen in the configuration space and shows quantum carpet evolution in the momentum space, a regime already observed in the experiment [10]. In the latter case of chaotic dynamics the BEC spreads sub-diffusively, with the second momentum growing approximately as $\sqrt{t}$. This latter regime deserves further studies because of its relation to the problem of quantum chaotic diffusion. Indeed, it has been known since the pioneering work [20] that quantum interference effects strongly modify the classical diffusion due to chaotic dynamics (the so-called phenomenon of dynamical localization [21]). Because the mean-field approach used in this work can be considered as a pseudo classical limit of the quantum many-body dynamics [11], it is very interesting to compare the above mean-field prediction with the behavior of the second momentum calculated on the basis of the Bose-Hubbard model, as well as that observed in a laboratory experiment.

Subsequent to the preparation of this paper we learned about recent work [22] where the authors address the same problem of different dynamical regimes in biased DNLSE, although with a different motivation. As initial conditions an extreme case of single site population was mostly considered. Among other regimes, a regime with no wave-packet spreading and one with sub-diffusive spreading, where $M(t) \sim t^{0.38}$, were reported. Taking into account that solutions of a nonlinear equation are typically sensitive (even asymptotically) to the type of initial conditions, results of the both papers may be considered as consistent.

Acknowledgments

Support from the Deutsche Forschungsgemeinschaft via the Graduiertenkolleg 'Nichtlineare Optik und Ultrakurzzeitphysik', Volkswagen Foundation, DAAD and Colciencias is gratefully acknowledged.

---

[1] B. P. Anderson and M. A. Kasevich, Science **282** (1998) 1686.

[2] O. Morsch, J. H. Müller, M. Cristiani, D. Ciampini, and E. Arimondo, Phys. Rev. Lett. **87** (2001) 140402.

[3] A. R. Kolovsky, Phys. Rev. Lett. **90** (2003) 213002; A. Buchleitner and A .R. Kolovsky, Phys. Rev. Lett. **91** (2003), 253002.

[4] A. R. Kolovsky, preprint: cond-mat/0412195 (2004).

[5] Yi Zheng, M. Kostrun, and J. Javanainen, Phys. Rev. Lett. **93** (2004) 230401.

[6] H. Ott, E. de Mirandes, F. Ferlaino, G. Roati, G. Modugno, and M. Inguscio, Phys. Rev. Lett. **92** (2004) 160601.

[7] D. Witthaut, M. Werder, S. Mossmann, and H. J. Korsch, Phys. Rev. E **71** (2005) 036625.

[8] M. Gustavsson, E. Haller, M. J. Mark, J. G. Danzl, G. Rojas-Kopeinig, and H.-C. Nägerl, Phys. Rev. Lett. **100** (2008) 080404.

[9] M. Fattori, C. DErrico, G. Roati, M. Zaccanti, M. Jona-Lasinio, M. Modugno, M. Inguscio, and G. Modugno, Phys. Rev. Lett. **100** (2008) 080405.

[10] M. Gustavsson, E. Haller, M. J. Mark, J. G. Danzl, R. Hart, A. J. Daley, and H.-C. Nägerl, arXiv 0812.4836 (2008).

[11] A. R. Kolovsky, E. M. Graefe, and H. J. Korsch, arXiv 0901.4719 (2009)

[12] M. V. Berry, J. Phys. A **29** (1996) 6617.

[13] M. V. Berry and S. Klein, J. Mod. Opt. **43** (1996) 2139.

[14] F. Grossmann, J. M. Rost, and W. P. Schleich, J. Phys. A **30** (1997) L277.

[15] P. Stifter, W. E. Lamb Jr., and W. P. Schleich, in *Frontiers of Quantum Optics and Laser Physics*, edited by Y. S. Zhu, M. S. Zubairy, and M. O. Scully. World Scientific, Singapore, 1997.

[16] M. V. Berry, J. Phys. A **32** (1999) L329.

[17] This does not imply that the Lyapunov exponent is strictly zero, i.e., one should not exclude a possibility that the quasi regular dynamics depicted in Fig.2 is also

a transient.

[18] A. R. Kolovsky, A. V. Ponomarev and H. J. Korsch, Phys. Rev. A **66** (2002) 053405.

[19] Ya. B. Zeldovich and A. S. Kompaneets, in *Collection in Honor of the Seventieth Birthday of Academician A. F. Ioffe*, page 61. Izdat. Akad. Nauk SSSR, Moscow, 1950.

[20] G. Casati, B. V. Chirikov, F. M. Izrailev, and J. Ford, in *Lecture Notes in Physics, Vol.93*, page 334. Springer, Berlin, 1979.

[21] H.-J. Stöckmann, *Quantum Chaos*, Cambridge University Press, Cambridge, 1999.

[22] D. O. Krimer, R. Khomeriki, and S. Flach, arXiv 0904.2867 (2009).